Chemical Papers (2021) 75:2945–2956
https://doi.org/10.1007/s11696-021-01547-5

ORIGINAL PAPER

Novel *n*-octadecylcarboxamide CoPc: amperometric detections for bioanalytes using modified GCE

Mounesh[1] · **K. R. Venugopal Reddy**[1] · **O. Nagaraja**[2]

Received: 14 July 2020 / Accepted: 29 January 2021 / Published online: 13 February 2021

Abstract

Here, we are reporting cobalt(II) phthalocyanine (CoPc) containing the active catalyst for the electrochemical investigations of bioanalytes. The synthesized tetra-*n*-octadecylcarboxamide cobalt(II) phthalocyanine was characterized by FT-IR, UV, TGA, mass and powder XRD analysis. In the present work, the synthesized complex was characterized by cyclic voltammetry and shows the redox behaviour corresponding to central metal (Co^{+II}/Co^{+I}) of the complex. Three biomolecules are well separated by their oxidation peaks in simultaneous detections of AA, DA and UA at 170, 350 and 550 mV with increasing high positive peak current. The low detection limit of AA, DA and UA was 40, 30 and 30 µmol by CV methods. The modified tetra substituted CoODAPc/GCE exhibits an excellent electrocatalytic activity, stability, high sensitivity, good linearity and selectivity without losing its catalytic activity and proves to be a versatile chemical sensor for commercial pharmaceutical samples, vitamin C tablets and dopamine injections.

✉ Mounesh
mounesh.m.nayak@gmail.com

[1] Department of Studies and Research in Chemistry, Vijayanagara Sri Krishnadevaraya University, Ballari-583105, Karnataka, India

[2] Department of Studies and Research in Chemistry Kuvempu University, Jnanasahyadri, Shankaragatta-577451, Karnataka, India

Graphic abstract

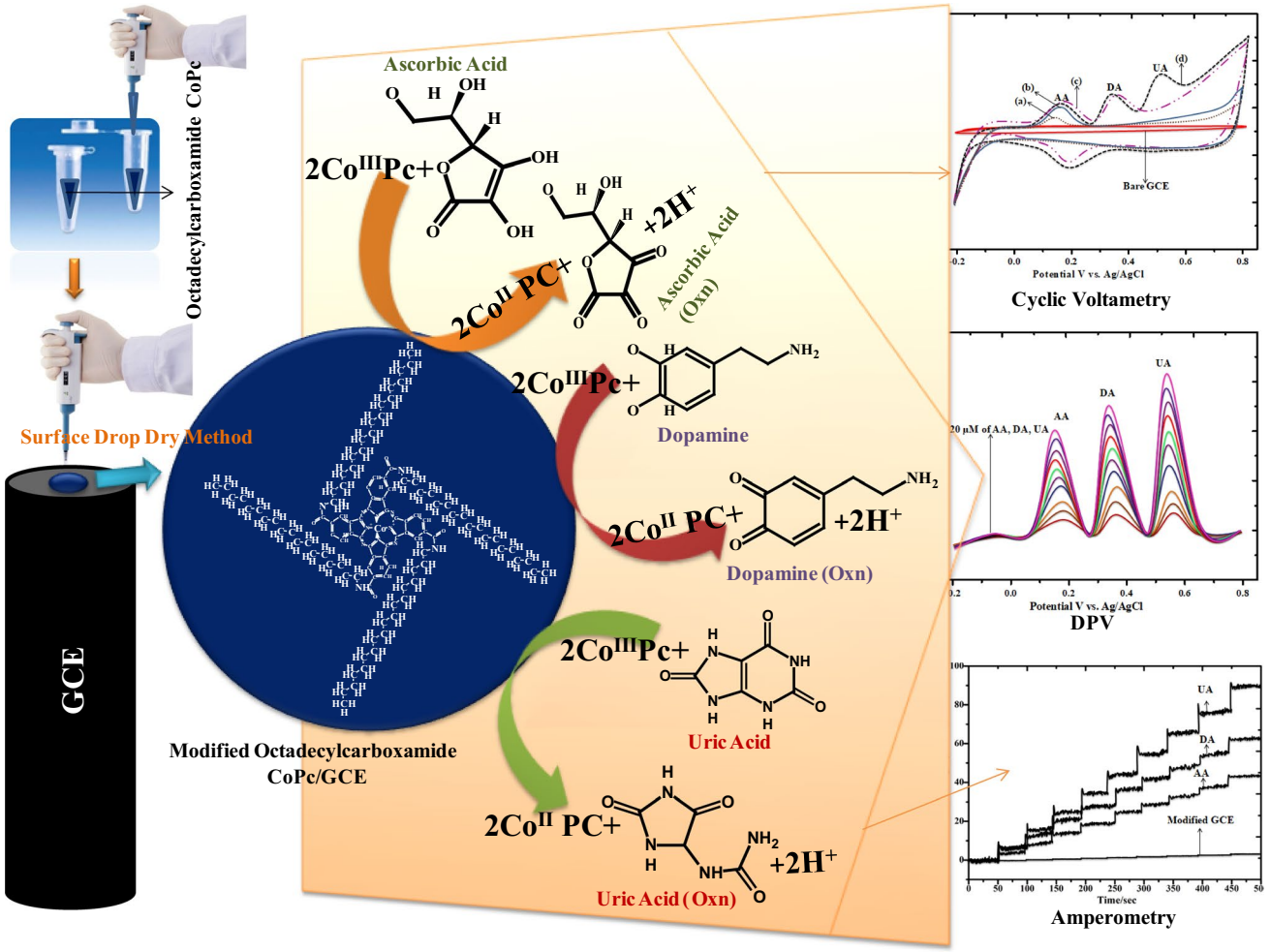

Keywords Sensors · Ascorbic acid · DCC · GCE · DA · UA · CoPc

Introduction

DA (3,4dihydroxyphenylethylamine) and other catecholamine play an important role in central nervous system, cardiovascular, renal and hormonal systems as well as in drug addiction and Parkinson disease (Salimi et al. 2006). Abnormal release of DA may relate to many diseases, such as Parkinson's disease, Huntington's disease, tardive dyskinesia and Alzheimer's diseases. AA also known as vitamin C exists widely in food, plant and animal tissues. Excess AA intake will lead to urinary stone, diarrhoea and stomach convulsion. UA is the purine and its metabolism product in the human body. The UA leads to several diseases (e.g. gout, allergic, rashes, prickly heat, hyperuricaemia and LeschNyhan syndrome). Therefore, it is essential to develop simple and rapid methods for the determination of these biological molecules in routine analysis. Several methods and catalytic materials have been used for the detection and sensing of these biomolecules (Colín-Orozco1 et al. 2012; Weihua et al. 2014; Ensafi Ali et al. 2009). The literature survey reveals that phthalocyanine was also used for the investigation and sensing of AA, DA and UA molecules (Mounesh et al. 2019a, b). Metallophthalocyanines (MPCs), with the planar 18 π-electron conjugated systems, are a well-known class of N4-macrocyclic metal compounds (Mounesh et al. 2020; Mounesh et al. 2020; Mounesh et al. 2020; Mounesh et al. 2020; Mounesh et al. 2021). In spite of their versatile electrochemical applications, a very less attention was paid towards the synthesis of octadecylamine derivatives containing macrocyclic moiety.

The present study was related to the synthesis of novel tetra-*n*-octadecylcarboxamide cobalt(II) phthalocyanine

(CoODAPc) containing macrocyclic moiety and explored the electrochemical investigations for analytes like AA, DA and UA. The CoTcPc complex substituted with octadecylamine (ODA) was expected to enhance the solubility of CoPc in organic solvents and tendency towards sensing of biomolecules in PBS (pH = 7) electrolyte. The modified CoTODAPc/GCE was used for micro-molar solution in simultaneous and individual detection of AA, DA and UA and interferences studies and real samples analysis using cyclic voltammetry (CV), differential pulse voltammetry (DPV) and chrono-amperometry (CA) techniques. The voltammograms of AA, DA and UA which are in the micro-molar solutions level concentrations and most suitable for biological fluids, food, plant and animal tissue in neutral PBS electrolyte solutions and for Vitamin 'C', dopamine hydrochloride injection and human urine real samples analysis.

Materials and methods

Instrumentations

Ultraviolet–visible (UV–Vis) absorption spectra were recorded on Shimadzu UV-2550 spectrophotometer and infrared spectra on Perkin-Elmer spectrum 100 FT-IR spectrometer. X-ray powder diffraction patterns were recorded using a Cu Kα radiation ($\lambda = 1.5405$ Å, nickel filter), on a Bruker D8 Discover equipped with a Lynx Eye detector. The data were obtained in the range of 2θ, 5–100°. The X-ray diffraction (XRD) analysis was carried out using Eva (evaluation curve fitting) software. Thermal gravimetric analysis (TGA) was recorded on a Shimadzu DTG-TG 60H with a gas flow of 120 ml/min and operated under nitrogen atmosphere. A mass spectrometry study of the final compound was confirmed by ESIMS MALDI-Micromass QTOF2 equipment. All the electrochemical measurements were carried out on a CHI620E electrochemical workstation USA with a conventional three-electrode system (glassy carbon electrode, platinum wire electrode and Ag/AgCl electrode).

Precursors

Octadecylamine (ODA) was procured from Sigma Aldrich. *N*,*N*′ dicyclohexylcarbodiimide, *N*,*N*′ dimethylformamide, potassium carbonate anhydrous were procured from spectrochem Pvt, Ltd. Dopamine was purchased from Hi-Media Laboratories Pvt, Ltd. (INDIA), ascorbic acid and uric acid were procured from SDFCL Ltd Co, (INDIA), and used without further purifications.

Synthesis of tetra-*n*-octadecylcarboxamide cobalt(II) phthalocyanine (CoODAPc) complex

Tetra-carboxy cobalt(II) phthalocyanine (CoTcPc) (1 g, 0.0013 mol), K_2CO_3 (0.92 g, 0.0066 mol) and N,N´ dicyclohexylcarbodiimide as catalyst was dissolved in dimethylformamide (DMF, 20 mL) with constant stirring for 20 min and the solution of octadecylamine (1.8 g, 0.0066 mol) was added slowly with stirring (Scheme S1). The reaction mixture was stirred for 48 h at room temperature. The reaction mixture was poured into ice cold water to yield dark green precipitate and further purified with hot water followed by hexane and dried over P_2O_5 in vacuum desiccator (Mounesh et al. 2020).

Yield: 87%. Mol. Wt.: 1753. IR (KBr, cm^{-1}): 3322 (–CONH), 2928–2846 (Ar–CH), 1625 (C=N), 1513 (C=C), 1452 (C–C), 1303, 1227, 1149, 1092, 893, 837, 629 cm^{-1} are attributed to the various skeletal vibration of PC ring (Fig. S1).

Preparation of modified electrode

The bare glassy carbon electrode was polished to mirror surface by gentle polishing sequentially with 0.3 and 0.05 µm alumina slurry on a Buehler polishing pad. Then, electrode was sonicated two times each in doubly distilled water and alcohols separately for 5 min to remove alumina particles trapped on the surface. The GCE rinsed with excess water, dried and kept in a desiccator. The green ink of CoTODAPc (5 mg CoTODAPc was suspended in 0.5 mL dry DMF solvent) was prepared ink was drop cast on the glassy carbon electrode and dried in room temperature.

Results and discussion

The synthesis of CoTODAPc complex was shown in Scheme S1. The amine group of *n*-octadecylamine is reacted with carboxylic group of CoTCPc to yield amide bridged tetra-*n*-octadecylcarboxamide cobalt(II) phthalocyanine (CoTODAPc). The elemental analysis data fairly agreed with the theoretical values indicating the synthesized complex is pure in nature. The CoTODAPc complex is blue coloured in nature and readily soluble in concentrated sulphuric acid and DMSO. The synthesized complex has been characterized by various spectroscopic as well as electrochemical techniques.

UV–Vis spectrum

The best indications for phthalocyanine systems are given by their UV–Vis spectra in solution. Two principle π–π* transitions are seen for PCs: a lower energy Q-band region (visible blue and red region) at around 650–700 nm, π–π* transition

from highest occupied molecular orbital (HOMO) to lowest unoccupied molecular orbital (LUMO) of the complexes and a higher energy B band region at around 300–400 nm, deeper π–π^* transition from the highest occupied MO's (Fig. 1 inset a and b curve) to the LUMO (Mounesh et al. 2020). The B bands within the UV range of 320–400 nm were due to the transitions from the deeper π levels to the LUMO (Fig. 1 inset a curve) a shoulder peak at 600–650 nm was observed in the Q-band region may be due to vibronic fine structure as well as presence of dimer and oligomeric complex species in solution. Hence, the absorption spectrum of this novel complex can be tuned for spectral shifts by varying the substituent attached to the CoTODAPc (Fig. 1 inset a curve) and CoTCPc (Fig. 1 inset b curve).

FT-IR spectra

IR spectral data clearly indicate the formation of compound by the appearance of new absorption bands at 3317–3322 cm^{-1} (–CONH), (–COOH) and (–NH2) Fig. S1a and b, 2840–2928 (Ar–CH), 1625–1628 cm^{-1} for C=N, 1513–523 cm^{-1} for C=C, 1450^{-1}452 cm^{-1} for C–C, 1313, 1227, 1086, 887, 837, 741, 636 are attributed to the various skeletal vibration signals of CoTCPc and CoTODAPc ring and substituted ligand for octadecylamine as shown in Fig. S1.

Thermal properties

The thermal stability of the bare CoTCPc and CoTODAPc was studied using TGA. Figure 2a, b illustrates typical TGA thermograms of weight loss as a function of temperature range from 100 to 800 °C. The sample (50 mg) was heated from room temperature to 800 °C at rate of 5 °C/min in nitrogen. The TGA curve (above) is labelled in terms of the identity of the complex. The temperature ranges from 100 to 400 °C (50% weight loss of substituted ligand), 400–570 °C (21% weight loss of Pc ring) Pc complex and 570–800 °C (29% weight loss of CoO). The degradation temperature was found to vary as a function of temperature. Figure 2b shows that the thermal stability of the CoTODAPc complex was higher than that of pure Pcs where the degradation temperature is significantly shifted to higher values (Fig. 2a) (Mounesh et al. 2019a, b; Jilani et al. 2020).

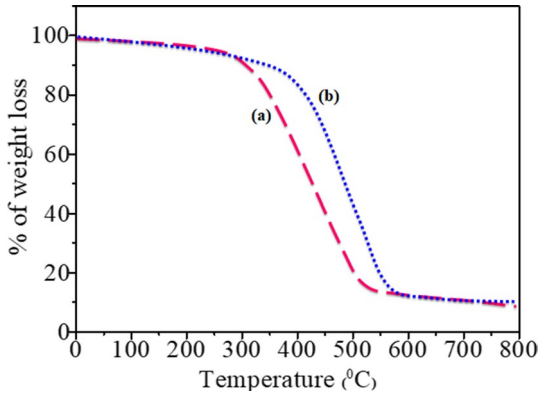

Fig. 2 TGA of **a** CoTCPc **b** CoTODAPc

X-ray diffraction analysis

X-ray powder diffraction (XRD) was employed to elucidate the crystal nature and size of the substituted CoPc. The patterns are qualitative and are similar to that of CoTODAPc; however, the pattern was more dispersive in intensity than the corresponding metal phthalocyanine. The XRD pattern was used to explain qualitatively the degree of crystallinity (Sawada et al. 2005; Mounesh et al. 2021). The XRD pattern indicates that the obtained CoTODAPc is amorphous in nature. The 8, 9, 15, 17, 18, 19, 21, 23, 26, 30 peaks that were observed at room temperature disappeared and four other lines emerged (Fig. 3). This peak corresponds to long

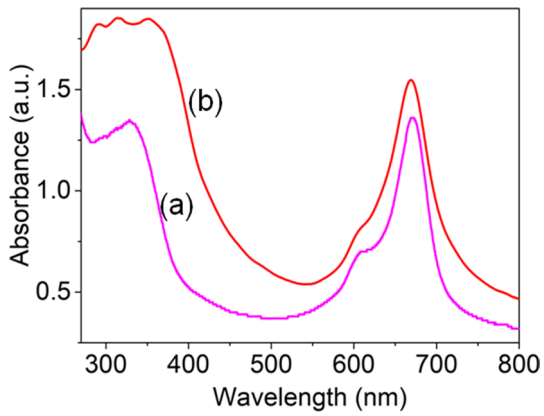

Fig. 1 UV–visible spectra of **a** CoTODAPc and **b** CoTCPc

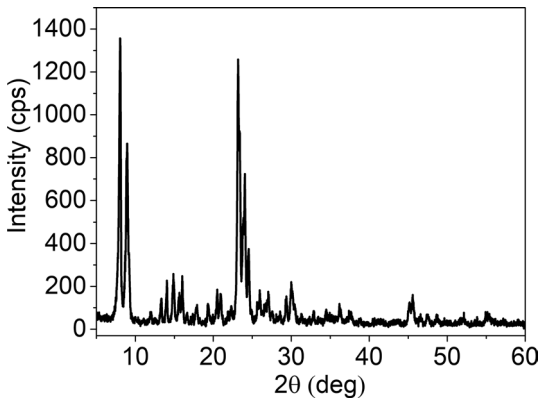

Fig. 3 X-ray diffractograms of CoTODAPc

aliphatic chains that are located randomly within the columnar mesosphere with an average spacing of 4.6 Å. A less broad peak was found around 3.4 Å, which was the stacking distance of phthalocyanine core within the columns. These results are similar to the data of the CoODAPc obtained (Sleven et al. 2001; Jilani et al. 2019). The observed patterns are very much similar to parent phthalocyanines except the broadening of the peaks. The broadening may be due to the presence of substituent and which seems to play an important role in the stacking of the substituted phthalocyanine derivative.

Mass spectrum

The ESI–MS mass spectrum of compound CoTODAPc is depicted in scheme S1 and confirmed the proposed structure. The molecular ion peaks at $m/z = 1753$; Mass: m/z = Found $(M+Z)$ 1754 (Fig. S2).

Electrochemical investigation of biomolecules

Simultaneous detections electrocatalytic oxidation for AA, DA and UA

Cyclic voltammogram for the oxidation of tetra CoTODAPc/GCE in PBS (pH = 7) electrolyte solution was utilized to assess the electrochemical sensing studies of AA, DA and UA by modified GC electrode. The bare GCE Fig. 4 (inset red curve) and CoTODAPc/GCE exhibit a peak at cathodic peak potential 120 mV and positive current Fig. 4 inset a curve. The 15 µM of AA is detecting the cathodic peak potential (130 mV) as shown in Fig. 4 inset b curve (Zucolotto et al. 2006), and 10 µM DA shows a cathodic peak at potential 350 mV (Fig. 4 inset c curve) with applied scan rate of 50 mV s^{-1}. Further, AA and DA keep at constant at same electrolyte solution in presence of UA (10 µM) is detecting cathodic peak potential 520 mV (Fig. 4 inset d curve), (Tsierkezos et al. 2016). DA is detecting the cathodic peak potential at 350 mV and three species were detection by three different peak potential as shown in Fig. 4 (Thiagarajan et al. 2007). Here, the CoTODAPc/GC electrode is highly electro-catalytically active towards three different potential peaks, sensitivity and selectivity, as shown in Table S1 (Zucolotto et al. 2006; Tsierkezos et al. 2016; Thiagarajan et al. 2007; Yanga et al. 2014).

Effects of Scan rates for AA, DA and UA

Fig. S3 shows the influence of different scan rate on CV response of AA, DA and UA at CoTODAPc/GCE. With the increase in scan rate from 10 to 100 mV/s, the anodic peak currents increase correspondingly. The scan rate of cyclic voltammetry exhibits a profound effect on the oxidation peak current of AA predicts the cathodic peak potential (170 mV) and increasing scan rates with increasing positive current (Fig. S3A), AA is displayed the linear responses, linear equation; $Y = 0.2035$ (AA) + 4.0414 with a correlation coefficient of $R^2 = 0.998$ (inset Fig. S3A). The AA inpresence DA is detecting the different cathodic peak potential, with increasing high positive peak current responded (Fig. S3B), and linear regression curve of peak current vs. various scan rate of AA and DA; $Y = 0.178$ (AA) + 5.293, $Y = 0.20$ (DA) + 6.178 with correlation coefficient of $R^2 = 0.999$ and 0.999 (inset Fig. S3B). When the scan rate increases in the range of 10–100 mV/s, simultaneous determinations of AA, DA and UA exhibit positive shifts in the three different oxidation peaks (Fig. S3C), suggesting that the adsorption of DA, UA and AA does not occur on CoTODAPc/GCE in PBS (pH7) solution. The redox peak currents do not increase as the scan rate increases, while a linear relationship is established between the positive peak current and the square root of scan rate. The linear equations are expressed as follows: AA: Ipa (µA) = 0.161 $\upsilon^{1/2}$ (mV s^{-1}) + 6.662, $R^2 = 0.999$; DA: Ipa (µA) = 0.163 $\upsilon^{1/2}$ (mV s^{-1}) + 8.488, $R^2 = 0.999$; UA: Ipa (µA) = 0.2272 $\upsilon^{1/2}$ (mV s^{-1}) + 12.754, $R^2 = 0.999$ (inset Fig. S3C); the above results indicate that the modified CoODAPc/GC electrode shows a highly electrocatalytic activity.

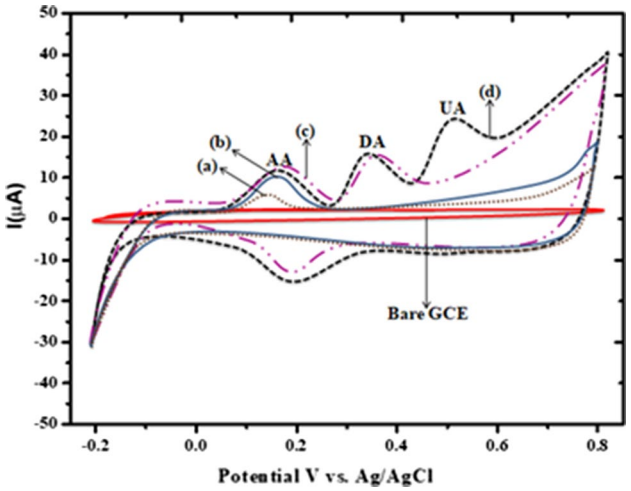

Fig. 4 Cyclic voltammograms plot of CoTODAPc/GCE in PBS (pH = 7) electrolyte solution at peaks; bare GCE (red curve), **a** modified GCE, **b** 15 µM of AA, **c** 10 µM for DA and **d** 10 µM for UA; At scan rate = 50 mV s^{-1}

DPV studies

The excellent electrocatalytic activity of CoTODAPc/GCE provides a substantial basis for simultaneous determination

of AA, DA and UA in PBS (pH 7) electrolyte solution. In these measurements, the concentration of the target biomolecule was only changed, while concentrations of the other two biomolecules were kept constant. Fig. S4C shows three peaks located at 170, 350 and 550 mV corresponding to the oxidation of AA, DA and UA that are well separated on the CoTODAPc. The peak currents of AA oxidation increase linearly in the range of 2–20 µM with the detection limit of 6×10^{-7} M in the presence of DA and UA. In addition, the successive addition of the AA into the electrochemical system (AA detecting the excellent cathodic peak potential (170 mV) as shown Fig. S4A) does not generate dramatic effects on the peak potentials of the DA and UA. The linear equation of AA is *I*p, $Y=1.630(AA)+7.228$, with the correlation coefficient of 0.999 (inset Fig. S4A). Similarly, in Fig. S4B and C, the oxidation peak currents of DA and UA increased linearly with the increase in their corresponding concentrations by keeping the concentrations of another biomolecule constant. Three species are detected with well-defined potential (170, 350 and 550 mV), having detection limits of 6, 5 and 1.67×10^{-7} M at $S/N=3$, respectively. The linear equations of DA and UA are *I*p, $Y=2.20(DA)+14.484$ (inset Fig. S4B) and *I*p, $Y=2.208(UA)$-0.177 (inset Fig. S4C) with the correlation coefficients of 0.999 and 0.999, respectively. These experimental results indicated that the simultaneous determination of the above three species was feasible in mixture using DPV method. In addition, all the parameters were listed for the three biomolecules in Table S1 (Wei et al. 2013; Yang et al. 2014; Yan et al. 2013; Chen et al. 2015; Zhao et al. 2016). Based on the presented results, we can conclude that the electrochemical sensor based on the CoTODAPc/GCE shows an attractive performance towards the simultaneous determination of AA, DA and UA.

The outstanding performance of the CoTODAPc/GC electrode was detecting the various concentrations of mixtures (AA, DA and UA) with detecting the three different positive potential (170, 350, 550 mV) as shown in Fig. 5A. The calibration curves of the peak currents were linear in the concentration ranges of 2–20 µM for AA, DA and UA. The linear equations of AA, DA and UA (Fig. 5B) were *I*p, $AA=2.04(AA)+2.30$, *I*p, $DA=2.5217(DA)+2.1553$ and *I*p, $UA=3.00(UA)+2.646$ with the correlation coefficients of 0.99854, 0.999 and 0.9939, respectively. These results demonstrate that the simultaneous determination of these biomolecules on CoTODAPc can be achieved with excellent sensitivity, good linear range and selectivity. Thus, CoTODAPc with unique structure and electrocatalytic properties represents a promising candidate for the construction of highly sensitive and selective biosensors, Table S1.

Amperometric determination of individual and interference studies

The CoTODAPc/GCE-based sensor was probed further using amperometric Fig. 6. Initially, only PBS (pH 7) was present in the cell. Stirring was initiated, the electrode was poised at selected working potential (0.300 V for AA, 0.500 V for DA and 0.500 V for UA, respectively) and aliquots (50 mL) of AA, DA or UA stock solution (with stock concentrations of 20 µM for AA, DA and UA) were added at 50 s intervals. Figure 6a shows the amperometric responses of CoTODAPc/GCE to the successive addition of AA, DA or UA into the PBS buffer. The CoTODAPc/

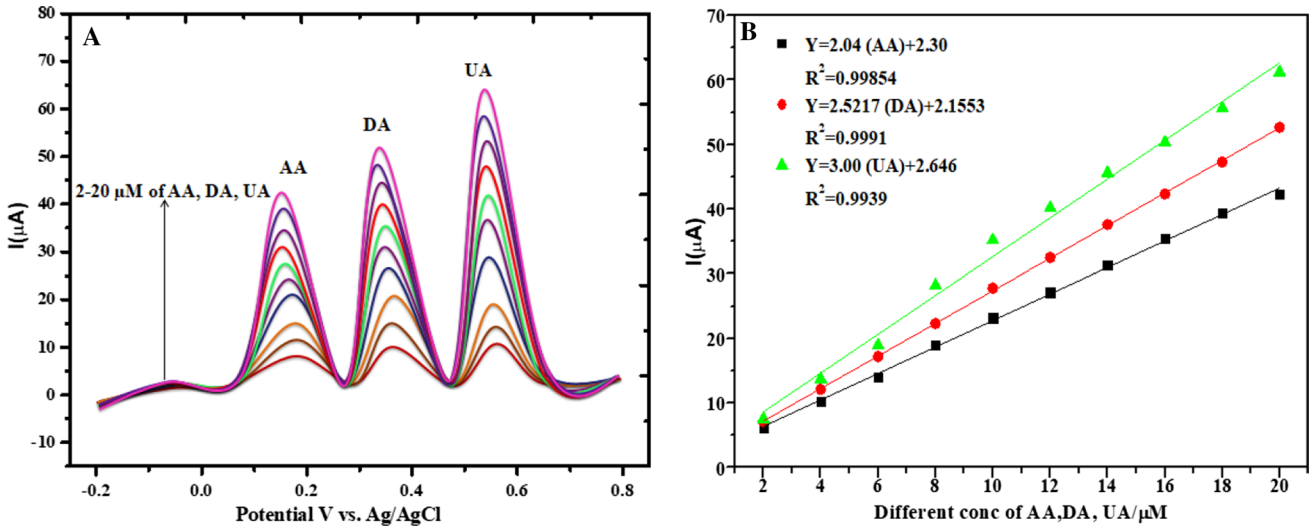

Fig. 5 Differential pulse voltammograms plot of CoTODAPc/GCE in PBS (pH = 7) electrolyte solution at peaks; **a** three mixtures determinations of different concentrations (2–20 µM) for AA, DA, UA/µM and **b** linear plot of cathodic peak current (Ipc) vs. different concentrations of AA, DA, UA/µM

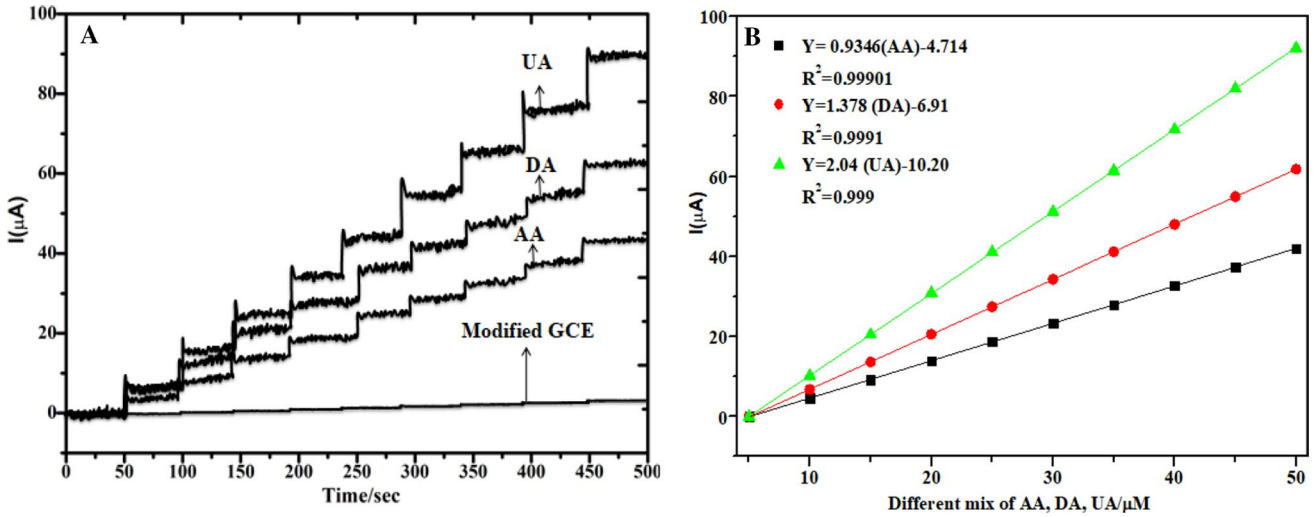

Fig. 6 Individual amperometric responses of CoTODAPc/GCE in PBS (pH = 7) electrolyte solution at peaks; **a** different amounts of (5–50 μL) for 20 μM AA, DA UA and **b** linear plot of cathodic peak current (Ipc) vs. different amounts of AA (black curve), DA (red curve), UA (green curve)

GCE electrode was found to exhibit linear response to additions of AA, or DA, or UA up to some concentration, after which the noise generated by stirring precluded the accurate measurement of the current. Inset Fig. 6b describes response of AA with addition of different amounts of 5–50 μL. The linear equation of Ipa with different amounts of AA (the inset in Fig. 6b black curve) was described as Ipa (μA) = 0.9346(AA)—4.7141, with correlation coefficient (R^2) of 0.999. The response range is 5 to 50 μM/L with a detection limit of 6×10^{-7} M at a signal-to-noise ratio (S/N) of 3 Table S1. Figure 6b depicts the amperometric response of DA at a fixed potential of 0.500 V. The linear equation (the inset in Fig. 6b red line curve) was presented as Ipa (μA) = 1.738 (DA)—6.91, ($R^2 = 0.999$), with a sensitivity of 1.738μA μM^{-1}. The response range is 5 to 50 μM with a detection limit of 5×10^{-7} μM ($S/N = 3$). In Fig. 6b (green line curve), the linear range could be observed between the current response and concentration of UA from 5 to 50 μM with a linear regression equation (the inset in Fig. 6B) *I*p (μA) = 2.04 (UA) – 10.04 ($R^2 = 0.9995$) (Fig. 6B green line curve). The sensitivity and detection limit are 2.04 μA μM^{-1} and 1.671×10^{-1} M ($S/N = 3$), respectively. Magnified portion of the amperometric response curve for addition of AA, DA or UA solution with very low concentration is shown in Fig. 6a (Shaopeng et al. 2015).

Selectivity studies

The selectivity of our catalyst (CoTODAPc/GCE) was studied in the presence of various interfering biochemicals like glucose, L-cysteine, tyrosine, H_2O_2 and glycine. Amperometric response for CoTODAPc/GCE on addition of AA, DA and UA in presence of different interfering compounds in PBS is shown in Fig. S5. An increase in amperometric current response was observed for the successful addition of 10 μM AA, DA and UA to the electrolyte containing interfering compounds. It was also observed that even after the addition of high concentration (10 μM) of the interference compounds like Glucose, L-Cysteine, Tyrosine, H_2O_2 and Glycine, did not have any significant response and also the interfering ions did not influence the AA, DA and UA detection. The addition of different interfering biochemical's in phosphate buffer solution did not influence the amperometric response for AA, DA and UA indicating the selective and superiority of the electrode (Saithip et al. 2014).

Individual detections

Detection of AA

The electrocatalytic activity of CoTODAPc modified GCE towards AA was investigated and results are shown in Fig. 7. In the absence of AA, oxidation peak current shifted to same potential observed by modified GCE at PBS (pH 7) electrolyte solution (Fig. 7a black line curve). After addition of different concentrations of AA from 5 to 25 μM, the oxidation peak current increases proportionally with increasing AA concentration. It demonstrated that the current response increase due to CoTODAPc can catalyze the oxidation of AA has good electrocatalytic activity towards AA oxidation. The electrocatalytic mechanism of AA on the GCE can be described by Eqs. (1), (2). CoPc (III) oxidizes AA to dehydroascorbic acid (DHAA) by the Co ion at the central of phthalocyanine structure and regenerates CoPc(II).

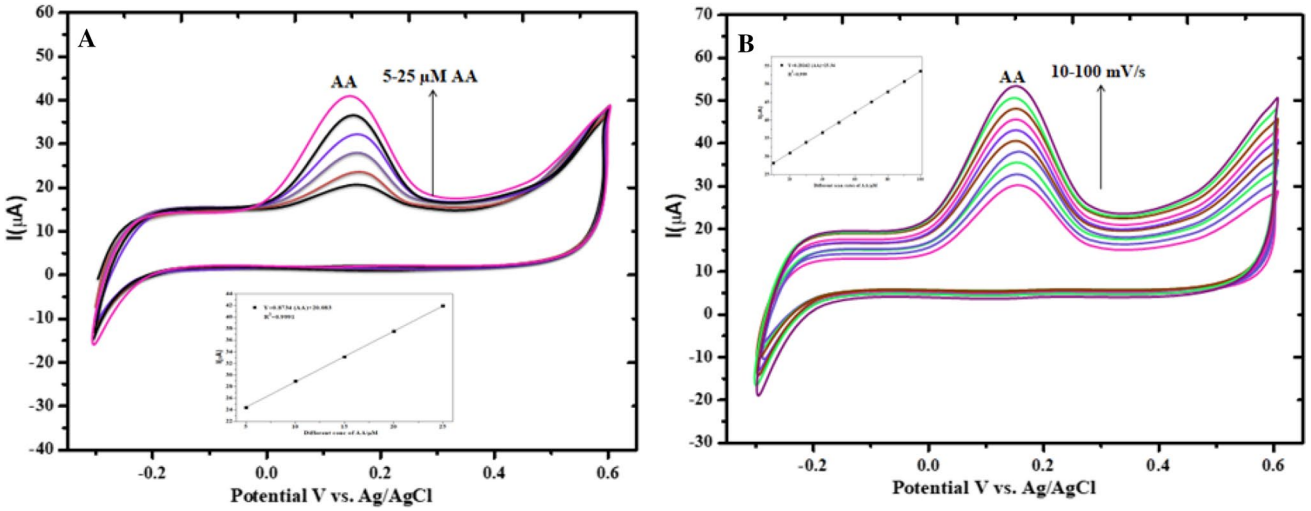

Fig. 7 Cyclic voltammograms plot of CoTODAPc/GCE in PBS (pH = 7) electrolyte solution at peaks; **a** modified GCE (black curve) and different concentrations of AA (2–25 µM); At scan rate 50 mV s^{-1} and **b** different scan rates of AA (10–100 mV s^{-1})

$$\mathrm{CoPc(II)} \leftrightarrow \mathrm{CoPc(III)} + e^{-} + H^{+} \quad (1)$$

$$2\mathrm{CoPc(III)} + \mathrm{AA} \rightarrow 2\mathrm{CoPc(II)} + \mathrm{DHAA} + 2H^{+} \quad (2)$$

The AA predicting the oxidation peak potential (170 mV) shows the linear responses of different concentrations on modified CoTODAPc/GCE, the linear regression equation; $Y = 0.8734\ (\mathrm{AA}) + 20.083$ with correlation coefficient of $R^2 = 0.9991$ (inset Fig. 7a). The different scan rates (10–100 mV/s) of AA display the well-defined linear and increases the scan rate with increasing positive current (Fig. 7b), while a linear relationship was established between the positive peak current and the square root of scan rate. The linear equations are expressed as follows: AA: Ipa (µA) = 0.28162 $\upsilon^{1/2}$ (mV s^{-1}) + 25.36, $R^2 = 0.999$ (inset Fig. 7b); the above results indicate that the oxidation of AA on CoTODAPc/GCE is a diffusion-controlled process and good linearity, reproducibility (Saithip et al. 2014; Zuo et al. 2012).

Detection of DA

The electrocatalytic activities of CoTODAPc modified GCE towards various concentrations of DA are depicted by cyclic voltammograms at a scan rate of 50 mV s^{-1}. Figure 8a displays the concentration dependence of DA at CoTODAPc/GC electrode. As expected, no redox peaks can be observed in pH 7 blank solution. After addition of different concentrations of DA from 5 to 25 µM, a well-defined and reversible pair of redox peaks located at 350 mV versus SCE appeared with the linear relationship between the peak currents and the different concentrations. The study suggests that the proposed sensor proved to be good electrocatalytic activity towards DA oxidation; the positive peak current of DA at CoTODAPc/GCE has a meagre increase than that of modified GCE (Fig. 8a black line curve). There were twofold increases in peak current with electrochemical process (ΔEp≈ 270 mV). A pair of well-defined redox peaks were also observed for CoTODAPc/GCE, indicating that the redox reaction of DA occurred at the electrode surface. The modified electrode was clear evidence of electrocatalytic effect towards DA oxidation (Łuczak et al. 2008; Huiying et al. 2006). The electrocatalytic mechanism of DA to the GCE can be described by Eqs. (3), (4). CoPc(III) oxidizes DA to dehydrodopamine (DHDA) by the Co ion at the central of phthalocyanine structure and regenerates CoPc(II).

$$\mathrm{CoPc(II)} \leftrightarrow \mathrm{CoPc(III)} + e^{-} + H^{+} \quad (3)$$

$$2\mathrm{CoPc(III)} + \mathrm{DA} \rightarrow 2\mathrm{CoPc(II)} + \mathrm{DHDA} + 2H^{+} \quad (4)$$

The linear response of CoTODAPc/GCE towards the different concentrations of DA vs. cathodic peak current (Ipc); $Y = 0.936(\mathrm{DA}) + 24.804$ with correlation coefficient of $R^2 = 0.999$ (inset Fig. 8). Figure 8b shows the different scan rates for DA with well-defined peak potential and intermediate peaks at same positive current and a linear relationship was established between the positive peak current and the square root of scan rate. The linear equations were expressed as follows: DA: Ipa (µA) = 0.28161 $\upsilon^{1/2}$ (mV s^{-1}) + 20.99152, $R^2 = 0.999$ (inset Fig. 8b); the above results indicate that the oxidation of DA on CoTODAPc/GCE was a diffusion-controlled process and good linearity,

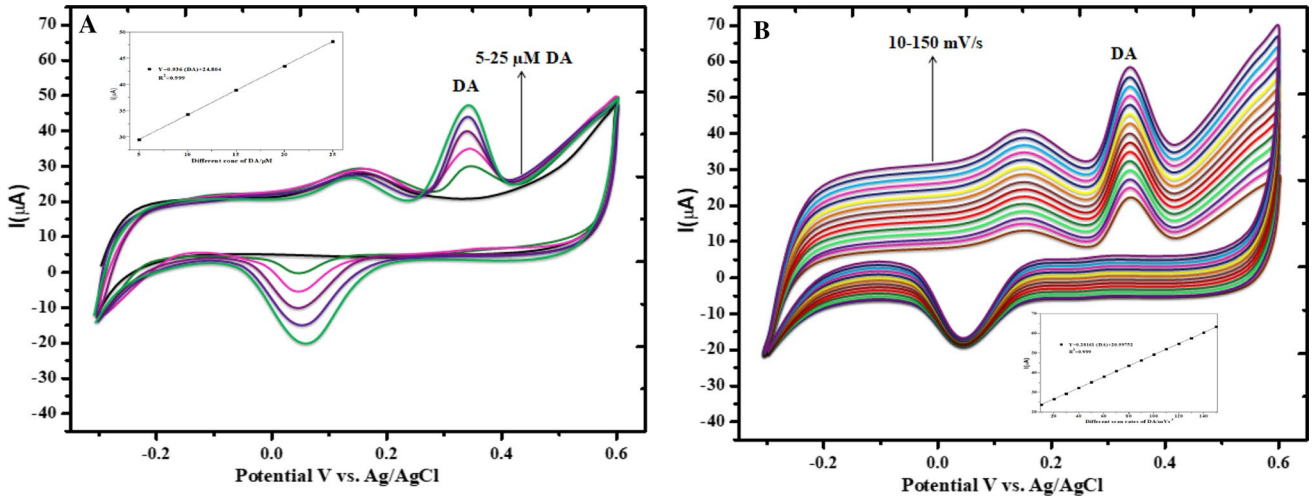

Fig. 8 Cyclic voltammograms plot of CoTODAPc/GCE in PBS (pH = 7) electrolyte solution at peaks; **a** modified GCE (black curve) and different concentrations of DA (2–25 µM); At scan rate 50 mV s^{-1} and **b** different scan rates of DA (10–150 mV s^{-1})

reproducibility and comparatively different literature of DA detection as shown in Table 1 (Wei et al. 2013; Cheng et al. 2012).

Detection of UA

Figure 9 shows the CVs plots for the modified CoTODAPc/GCE at PBS (pH 7) electrolyte at different concentrations (5–25 µM) of UA (Fig. 9a) predicting the well-defined cathodic peak potential (550 mV) and there was a linearity with concentration of UA. The UA could be electrochemically quantified when they are not mixed with another analytes. The linearity of UA; $Y = 1.1678\ (UA) + 24.985$ with correlation coefficient and sensitivity $R^2 = 0.999$ and 1.1678 µA µM/L (inset Fig. 9a). The analytic parameters namely: linearity range, sensitivity, detection (DOL) and quantification limits (QOL) were shown in Table S1. The observed results with the modified GCE (Fig. 9a black line curve) were more sensitive towards the UA. Figure 9b shows the increasing scan rates with increasing peak current (Ip)(10–100 mV/s), while a linear relationship was established between the positive peak current and the square root of scan rate. The linear equations were expressed as follows: UA: Ipa (µA) = 0.40217 $\upsilon^{1/2}$ (mV s^{-1}) + 22.12667, $R^2 = 0.999$ (inset Fig. 9b); the above results indicate that the oxidation of UA on CoTODAPc/GCE was a diffusion-controlled process with good linearity, reproducibility, low detection limit for UA.

Table 1 Comparative study of CoTODAPc/MWCNTs/GCE modified electrode with other modified electrodes in the detection of dopamine

Sl. no	Modified electrodes	Method	LOD	Sensitivity	References
1	[a]AuNPs@SiO2-MIP sensor	CV	200 nM	4.8 µA nM L^{-1} cm^{-2}	Yu et al. (2012)
2	[b]PDEs-PAD	CV	0.04 µM	6.91 nA µM L^{-1} cm^{-2}	Weibo et al. (2016)
3	[c]GCE/MWCNT/β-CD	CV	6.7 µM	116.63 nA mM L^{-1} cm^{-2}	Alarco-Angeles et al. (2008)
4	[d]GNF/GCE	DPV	0.2 µM	0.022 µA µM L^{-1} cm^{-2}	Zheng et al. (2013)
5	[e]GNPs/MWCNTs	SWV	0.07 µM	2.06 µA µM L^{-1} cm^{-2}	Fabio et al. (2017)
6	[f]AuNPs/Ch/GCE	DPV	0.12 µM	1.741 µA µM L^{-1} cm^{-2}	Wang et al. (2007)
7	CoTODAPc/MWCNTs/GCE	CV	40 nM	0.045 µA nM L^{-1} cm^{-2}	This Work
		DPV	30 nM	0.065 µA nM L^{-1} cm^{-2}	
		CA	30 nM	0.154 µA nM L^{-1} cm^{-2}	

[a]AuNPs@SiO2-MIP, Gold nanoparticles @ silicon dioxide molecularly imprinted polymer microsensor; PDEs-PAD, pencil-drawn electrodes; [c]GCE/MWCNT/β-CD, β-cyclodextrin/multiwalled carbon nanotubes/GCE; [d]GNF, Gold nanoflower; [e]GNPs/MWCNTs, Gold nanoparticles with multiwalled carbon nanotubes; [f]AuNPs/Ch/GCE, gold nanoparticles/Choline; CA, Chrono-amperometry

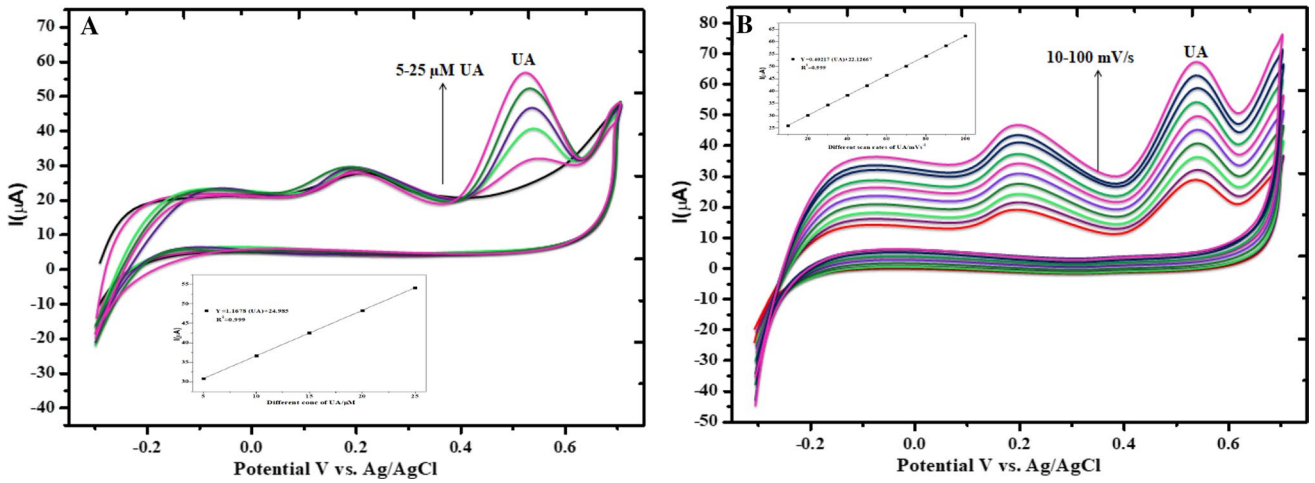

Fig. 9 Cyclic voltammograms plot of CoTODAPc/GCE in PBS (pH = 7) electrolyte solution at peaks; **a** modified GCE (black curve) and different concentrations of UA (2–25 µM); At scan rate 50 mV s^{-1} and **a** different scan rates of UA (10–100 mV s^{-1})

Determination of real sample analysis

Determination of AA in vitamin 'C' tablets

Vitamin 'C' tablet, containing 200 mg $tablet^{-1}$ AA, was finely powdered and accurately weighed and dissolved in 100 mL of water. The mixture was shaken for 20 min and filtered into a 100 mL volumetric flask. The residue was washed several times with water and the solution was diluted to the mark. 10 µL of the sample was diluted to 10 mL with PBS (pH 7) and then transferred to an electrolytic cell for the determination of AA by CoTODAPc/GCE. The vitamin C tablets of AA were analysed by the standard addition method, Table S2.

Determination of DA in dopamine hydrochloride injections

In order to verify the reliability of the method for analysis of DA in pharmaceutical product, this CoTODAPc/GCE was used to determine DA in dopamine hydrochloride injection (10 mg mL^{-1}, 2 mL per injection). 25 µL of the dopamine hydrochloride injection solution was injected into a 10 mL volume flask and made up to volume with PBS (pH 7). Then, this test solution was placed in an electrochemical cell for the determination of DA using DPV method. The analytical results are listed in Table S2. The results were satisfactory, showing that the proposed methods could be efficiently used for the determination of DA in injections.

Determination of UA in human urine sample

The utilization of the proposed method for real sample analysis was also investigated by direct analysis of UA in human urine sample. In order to fit into the linear range of UA, the 30 and 40 µM urine samples used for detection were diluted two times with PBS (pH 7). The results are listed in Table S2. The recovery of the spiked samples ranged between 96.7% indicating the detection procedures are free from interferences of the urine sample matrix.

Conclusion

In conclusion, a new CoTODAPc macromolecule was synthesized and characterized by FT-IR, UV–Vis and MASS spectra, electronic spectroscopy XRD and TGA. The obtained compounds show maximum visible light absorption from 200 to 700 nm and exhibit improved thermal stability. The electrochemical sensor exhibits high electrochemical sensing activity towards the detection of AA, DA and UA with well-separated oxidation potentials. The constructed sensor displays low detection limits, wide linear ranges and outstanding sensing performance towards the detection of AA, DA and UA. The CoTODAPc/GCE manifests an interesting potential as the candidate for the construction of electrochemical sensor for simultaneous detection of AA, DA and UA, and determinations of real samples analysis of AA in vitamin "C" tablet, DA in dopamine hydrochloride injections and human urine in UA. The proposed sensor is useful and suitable for the direct simultaneous determination of AA, DA and UA in real samples by means of the DPV.

Supplementary Information The online version contains supplementary material available at https://doi.org/10.1007/s11696-021-01547-5.

Acknowledgement One of the authors Mounesh thankful for financially support by the Vijayanagara Sri Krishnadevaraya University SC.ST fellowship.

Compliance with ethical standards

Conflict of interest The authors declare that they have no conflict of interest.

References

Alarcon-Angeles G, Perez-Lopez B, Palomar-Pardave M, Ramırez-Silva MT, Alegret S, Merkoci A (2008) Enhanced host–guest electrochemical recognition of dopamine using cyclodextrin in the presence of carbon nanotubes. Carbon 46:898–906

Chen LX, Zheng JN, Wang AJ, Wu LJ, Chen JR, Feng JJ (2015) Facile synthesis of porous bimetallic alloyed PdAgnanoflowers supported on reduced graphene oxide for simultaneous detection of ascorbic acid, dopamine, and uric acid. J Anal 140:3183–3192

Cheng HM, Qiu HX, Zhu ZW, Li MX, Shi ZJ (2012) Investigation of the electrochemical behavior of dopamine at electrodes modified with ferrocene-filled double-walled carbon nanotubes. J Electrochim Acta 63:83–88

Colín-Orozco E, Corona-Avendaño S, Ramírez-Silva MT, Romero-Romo M, Palomar-Pardavé M (2012) On the electrochemical oxidation of dopamine, ascorbic acid and uric acid onto a bare carbon paste electrode from a 0.1 M NaCl aqueous solution at pH 7. Int J Electrochem Sci 7:6097–6105

Ensafi Ali A, Taei M, Khayamian T (2009) A differential pulse voltammetric method for simultaneous determination of ascorbic acid, dopamine, and uric acid using poly (3-(5-chloro-2-hydroxyphenylazo)-4,5-dihydroxynaphthalene-2,7-disulfonic acid) film modified glassy carbon electrode. J Electroanal Chem 633:212–220

Fabio RC, Leticia BF, Aldo JGZ, Márcio FB, Luiz HM-J (2017) Gold nanoparticles supported on multi-walled carbon nanotubes produced by biphasic modified method and dopamine sensing application. Sens Actuators B chem 243:43–50

Huiying X, Jingjing X, Ling Y, Zhu L, Baohong L (2006) An electrochemical sensor for selective detection of dopamine based on nickel tetrasulfonated phthalocyanine functionalized nitrogen-doped graphene nanocomposites. J Electroanal Chem 779:92–98

Jilani BS, Mounesh MP, Mruthyunjayachari CD, Venugopala Reddy KR (2020) Cobalt(II) tetra methyl-quinoline oxy bridged phthalocyanine carbon nano particles modified glassy carbon electrode for sensing nitrite: a voltammetric study. Mater Chem Phys 239:121920

Jilani BS, Mruthyunjayachari CD, Malathesh P, Mounesh STM, Venugopala Reddy KR (2019) Electrochemical sensing based MWCNT-Cobalt tetra substituted sorbaamide phthalocyanine onto the glassy carbon electrode towards the determination of 2-amino phenol: a voltammetric study. Sens Actuators B Chem 301:127078

Łuczak T (2008) Preparation and characterization of the dopamine film electrochemically deposited on gold template and its applications for dopamine sensing in aqueous solution. J Electrochim Acta 53:5725–5731

Mounesh JBS, Malatesh P, Venugopala Reddy KR, Lokesh KS (2019a) Simultaneous and sensitive detection of ascorbic acid in presence of dopamine using MWCNTs-decorated cobalt(II) phthalocyanine modified GCE. Microchem J 147:755–763

Mounesh MP, Praveen Kumara NY, Jilani BS, Mruthyunjayachari CD, Venugopala Reddy KR (2019b) Synthesis and characterization of tetra-ganciclovir cobalt(II) phthalocyanine for electroanalytical applications of AA/DA/UA. J Heliyon 5:e01946

Mounesh Sharan Kumar TM, Praveen Kumar NY, Venugopal Reddy KR (2020) Poly (L-lactide)-carboxamide-CoPc with composite MWCNTs on glassy carbon electrode sensitive detection of hydrazine and L-cysteine. Anal Chem Lett 10(5):620–635

Mounesh Venugopala Reddy KR (2020a) Detection of nanomolar concentrations H_2O_2 Using cobalt(II) phthalocyanine modified GCE with MWCNTs. Ana Chem Lett 10(1):33–48

Mounesh Venugopala Reddy KR (2020b) Electrochemical investigation of modified GCE on carboxamide-PEG_2-biotin-CoPc using composite MWCNTs: sensitive detection for glucose and hydrogen peroxide. New J Chem 44(8):3330–3340

Mounesh Venugopala Reddy KR (2020c) Novel garnished cobalt(II) phthalocyanine with MWCNTs on modified GCE: sensitive and reliable electrochemical investigation of paracetamol and dopamine. New J Chem 44:16831–16844

Mounesh Venugopala Reddy KR (2020d) Novel Tetracinnamide cobalt(II) phthalocyanine immobilized on MWCNTs for amperometic sensing of glucose. Anal Chem Lett 10(2):137–151

Mounesh Venugopala Reddy KR (2020e) Sensitive and reliable electrochemical detection of nitrite and H_2O_2 Embellish-CoPc coupled with appliance of composite MWCNTs. Anal Chim Acta 1108:98–107

Mounesh Venugopala Reddy KR (2021) Decorated CoPc with appliance of MWCNTs on GCE: sensitive and reliable electrochemical investigation of heavy metals. Microchem J 160:105610

Saithip P, Johannes PM, Ditsayut P, Tanom L, Adisorn T (2014) Highly selective electrochemical sensor for ascorbic acid based on a novel hybrid graphene-copper phthalocyanine-polyaniline nanocomposites. J Electrochim Acta 133:294–301

Salimi A, Khezri M, Hallaj HR, Salimi A, MamKhezri H, Hallaj R (2006) Simultaneous determination of ascorbic acid, uric acid and neurotransmitters with a carbon ceramic electrode prepared by sol–gel technique. Talanta 70:823–832

Sawada K, Duan W, Sekitani K, Satoh K (2005) Polymerization and complex formation of phthalocyanine substituted by trioxyethylene in solution. J Mol Liq 119:171–176

Shaopeng Q, Bo Z, Heqing T, Xiaoqing J (2015) Determination of ascorbic acid, dopamine, and uric acid by a novel electrochemical sensor based on pristine graphene. J Electrochim Acta 161:395–402

Sleven J, Görller-Walrand C, Binnemans K (2001) Synthesis, spectral and mesomorphic properties of octa-alkoxy substituted phthalocyanine ligands and lanthanide complexes. Mater Sci Eng C 18:229–238

Thiagarajan S, Chen SM (2007) Preparation and characterization of PtAu hybrid film modified electrodes and their use in simultaneous determination of dopamine, ascorbic acid and uric acid. J Talanta 74:212–222

Tsierkezos NG, Othman SH, Ritter U, Hafermann L, Knauer A, Köhler JM, Downing C, McCarthy EK (2016) Electrochemical analysis of ascorbic acid, dopamine, and uric acid on nobel metal modified nitrogen-doped carbon nanotubes. Sens Actuators B 231:218–229

Wang P, Li Y, Huang X, Wang L (2007) Fabrication of layer-by-layer modified multilayer films containing choline and gold nanoparticles and its sensing application for electrochemical determination of dopamine and uric acid. Talanta 73:431–437

Wei Z, Wenjie Z, Shuang L, Huiyuan M, Chen W, Haijun P (2013) Fabrication and electrochemical sensing performance of a composite film containing a phosphovanadomolybdate and cobalt(II) tetrasulfonate phthalocyanine. Sens Actuators B 181:773–781

Weibo L, Dongping Q, Yubin L, Ning B, Haiying G, Chunmei Y (2016) Fully-drawn pencil-on-paper sensors for electroanalysis of dopamine. J Electroanl Chem 769:72–79

Weihua C, Ting L, Haijun D, Jianshan Y (2014) Electrochemical determination of ascorbic acid, dopamine and uric acid based on an exfoliated graphite paper electrode: a high performance flexible sensor. J Sens Actuators B 193:492–500

Yan J, Liu S, Zhang Z, He G, Zhou P, Liang H, Tian L, Zhou X, Jiang H (2013) Simultaneous electrochemical detection of ascorbic acid, dopamine and uric acid based on graphene anchored with Pd–Pt nanoparticles. J Colloid Surface B 111:392–397

Yang YJ, Li WK (2014) CTAB functionalized graphene oxide/multiwalled carbon nanotube composite modified electrode for the simultaneous determination of ascorbic acid, dopamine, uric acid and nitrite. J Biosens Bioelectron 56:300–306

Yanga Lu, Liua D, Huang J, Youa T (2014) Simultaneous determination of dopamine, ascorbic acid and uric acid at electrochemically reduced graphene oxide modified electrode. Sens Actuators B 193:166–172

Yu D, Zeng Y, Qi Y, Zhou T, Shi G (2012) A novel electrochemical sensor for determination of dopamine based on AuNPs@SiO2 core-shell imprinted composite. Biosens Bioelectron 8:270–277

Zhao D, Yu G, Tian K, Xu C (2016) A highly sensitive and stable electrochemical sensor for simultaneous detection towards ascorbic acid, dopamine, and uric acid based on the hierarchical nanoporous PtTi alloy. J Biosens Bioelectron 86:119–126

Zheng Y, Huang Z, Zhao C, Weng S, Zheng W, Lin X (2013) A gold electrode with a flower-like gold nanostructure for simultaneous determination of dopamine and ascorbic acid. Microchim Acta 180:537–544

Zucolotto V, Ferreira M, Cordeiro MR, Constantino CJL, Moreira WC, Oliveira ON (2006) Nanoscale processing of polyaniline and phthalocyanines for sensing applications. Sens Actuators B Chem 113:809–815

Zuo X, Zhang H, Nan L (2012) An electrochemical biosensor for determination of ascorbic acid by cobalt(II) phthalocyanine—multiwalled carbon nanotubes modified glassy carbon electrode. J Sens Actuators B Chem 161:1074–1079